Orifice Meters With Supercritical Compressible Flow[1]

By R. G. CUNNINGHAM,[2] CHICAGO, ILL.

The discharge characteristics of orifices at low pressure ratios were investigated. Probe measurements of high-velocity jets confirm and extend the work of Stanton. Expansion factors (Y) at pressure ratios down to $r = 0.13$ were measured for the flow of air in a 2-in. pipe meter and for the flow of steam in a 3-in. pipe meter. Both meters were installed in accordance with ASME specifications, and operated at a diameter ratio of 0.15. The effects of high approach velocity on the discharge characteristics of square-edged orifices at low pressure ratios were investigated; expansion factors were determined for diameter ratios from 0.2 to 0.8 over a range of pressure ratios from unity to 0.2. A linear Y-r correlation is shown to exist at low pressure ratios; a change of flow regime occurs at a pressure ratio of 0.63. A theoretical solution for supercritical flow, previously established by the author, is further compared with experimental results.

Nomenclature

The following nomenclature is used in the paper:

Subscripts

- 1 = position of undisturbed flow upstream from orifice
- 2 = discharge region
- o = orifice plate, circular opening

Symbols

- A = area
- C_p = specific heat at constant pressure
- C_v = specific heat at constant volume
- d = diameter
- d_o = orifice diameter, in.
- E = ASME thermal expansion factor for orifice plates
- F = Fahrenheit degrees
- ft = feet
- G = mass flow rate, lb per sec
- g_c = gravitational constant, lb_m ft/lb_f sec^2
- h = enthalpy per pound of fluid
- K = orifice discharge coefficient for incompressible flow
- lb_f = pound force
- lb_m = pound mass
- L = edge width of orifice
- m = orifice-meter area ratio $A_o/A_1 = \beta^2$
- p = pressure
- p_c = theoretical critical pressure
- p_{1c} = orifice initial pressure at corner tap
- p_{1w} = orifice initial pressure at wall tap
- p_{2c} = orifice discharge pressure at corner tap
- p_{2w} = orifice discharge pressure at wall tap
- R = gas constant, ft $lb_f/lb_m F$ abs
- r = pressure ratio p_2/p_1
- r_c = theoretical critical pressure ratio
- t = temperature
- T = absolute temperature
- v = specific volume
- w = velocity
- Y = orifice-meter expansion factor
- Y_{th} = theoretical expansion factor
- β = orifice-meter diameter ratio d_o/d_1
- γ = ratio of specific heats C_p/C_v
- Δp = orifice pressure difference $(p_1 - p_2)$
- ϵ = Regeln orifice-meter expansion factor
- μ = orifice-jet contraction coefficient for incompressible flow
- μ_o = orifice-jet contraction coefficient for compressible flow
- ρ = density $(1/v)$

Introduction

One-dimensional gas-dynamics relations may be developed which express the velocity of a compressible fluid at a certain cross section of the stream tube as a function of the ratio of the pressure at that section to the initial pressure. When the pressure ratio is that defined as the "critical," the fluid velocity is equal to the local velocity of sound, and the area is a minimum.

One-dimensional relations are commonly applied to the case of compressible flow through a nozzle, and the mass flow rate depends on the ratio of the downstream or receiver pressure to the initial pressure. Experiment reveals that the flow rate of a convergent nozzle attains constancy at a pressure ratio defined as the "maximum flow ratio." For a well-formed convergent nozzle, the (experimental) maximum flow ratio is essentially identical with the (theoretical) critical-pressure ratio. Evidently the occurrence of sonic velocity at the throat of the nozzle prevents flow response to changes in the discharge pressure.

Contrary to the behavior of the convergent nozzle, the square-edged orifice does not exhibit a maximum flow ratio. Rather, experiment shows that the flow rate (for constant upstream conditions) continues to increase at all pressure ratios between the critical and zero; this range is defined as the "supercritical" range of ratios.

One of the most widely used means of metering compressible fluids is the square-edged orifice. However, the flow characteristics of this metering device are comparatively unknown in the supercritical range of pressure ratios. The purposes of this investigation are (*a*) to establish the factors affecting supercritical flow, (*b*) to extend the present range of experimentally determined discharge coefficients for certain standard orifice meters to low pressure ratios, and (*c*) to investigate the effect of high velocities of approach on the supercritical flow characteristics.

The Orifice Jet at Supercritical Pressure Ratios

Stanton (1)[3] investigated the free jets issuing from sharp-edged orifices by means of total and static-head pressure probes. His findings may be summarized as follows:

[1] From certain experimental portions of a dissertation submitted to the graduate school of Northwestern University in partial fulfillment of the requirements for the degree of Doctor of Philosophy.

[2] Research Engineer, The Pure Oil Company, Research and Development Laboratories. Present position, Project Engineer, Engineering Experiment Station, The Pennsylvania State College, State College, Pa. Jun. ASME.

Contributed by the Fluid Meters Research Committee and Industrial Instruments and Regulators Division and presented at the Annual Meeting, New York, N. Y., Nov. 26-Dec. 1, 1950, of The American Society of Mechanical Engineers.

Note: Statements and opinions advanced in papers are to be understood as individual expressions of their authors and not those of the Society. Manuscript received at ASME Headquarters on August 12, 1950. Paper No. 50—A-45.

[3] Numbers in parentheses refer to the Bibliography at end of paper.

1 For supercritical flow, the orifice jet converged to a minimum section and then diverged.

2 The minimum area of the jet was found to be a function of the downstream pressure. As the pressure ratio was decreased, the minimum area approached the orifice and became larger.

3 The location of the critical axial pressure approximately coincided with the minimum section of the jet; and it shifted toward the orifice in the same manner as the minimum stream section as the pressure ratio was lowered.

Bailey (2) made an axial traverse of the static pressure along the flow axis in a $^1/_4$-in-diam convergent nozzle, and in a similar-sized orifice. Curves showing the drop in pressure in the direction of flow were plotted for a distance of nearly 2 diameters downstream and well-developed shock fronts were apparent for both the nozzle and the orifice.

The results of Stanton's investigation contribute greatly toward an understanding of high-velocity orifice flow; at the same time, several questions present themselves:

1 Are Stanton's results applicable to the jet issuing from an orifice having an unrestricted approach section?

2 What are the pressure-drop characteristics of an orifice jet for constant initial conditions and variable discharge pressures?

3 Do shock discontinuities originate at the edge of the orifice as in the case of nozzles?

4 At what pressure ratio do shock waves first appear in the orifice jet?

Answers to these questions are indicated in the following paragraphs.

An investigation of the orifice jet was made by more or less repeating Stanton's work, the important difference being that the orifice had a long and unrestricted approach section. The limitations of space prevent a review of the results (see reference 3); suffice it to point out that the pressure curves were quite similar to Stanton's. Shock disturbances were evident at all orifice pressure ratios below the critical; the closest approach to the orifice plates was of the order of one-half orifice diameter. Condensation shocks were detected in the free jet at positions determined by the initial humidity of the air and downstream from the critical jet-pressure location.

To study the effects of discharge pressure on a jet issuing from an orifice at supercritical pressure ratios, a discharge chamber with an adjustable axial probe guide was constructed. For a constant upstream pressure of 82 psia and an initial temperature of about 75 F, the pressure drop along the jet axis is shown in Fig. 1 for nine orifice pressure ratios. The critical pressure has the same value for all of the curves but not the same position, and the shift of p_c toward the orifice plate, as the discharge pressure is lowered, is readily apparent. The curves further reveal that the free jet develops shock waves for an orifice pressure ratio of 0.49, but not for a ratio of 0.535. Thus it would appear, that like the convergent nozzle, shock waves first originate in the free jet for a pressure ratio near the critical value.

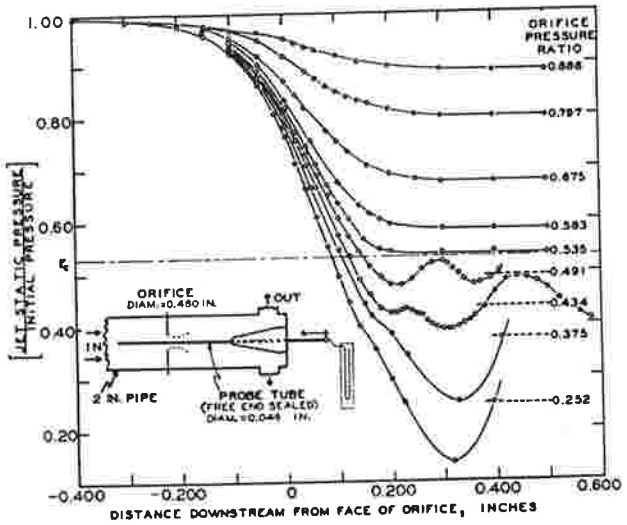

FIG. 1 STATIC-PRESSURE TRAVERSES ALONG AXES OF AIR JETS ISSUING FROM A SQUARE-EDGED ORIFICE

(Initial pressure 81.4 psia, initial temperature 75–79 F. Inset shows orifice plate and probe arrangement.)

A brief pressure-probe investigation of steam jets issuing from a square-edged orifice was made. The results were similar to those obtained with air. The critical jet pressure shifted toward the orifice as the discharge pressure was lowered. The high-velocity jet overexpanded and developed shock waves similar to those found in the jet from a nozzle. Shock disturbances first appeared in the orifice jet at pressure ratios quite near the critical value and the regular spacings of the shock fronts varied with the orifice pressure ratio.

EXPERIMENTAL INVESTIGATION OF ORIFICE METERING

The laboratory investigation of orifice metering was divided into separate phases:

(*a*) An extension of the present range of the ASME orifice expansion factors (4).

(*b*) An investigation of the effects of high velocity of approach on the supercritical flow characteristics of an orifice meter.

The equation

$$G = KY A_o \sqrt{2g_c \rho_1 \Delta p} \quad \ldots\ldots\ldots\ldots [1]$$

hereafter referred to as the "ASME Equation" (4), was adopted as the basic experimental flow equation. The discharge coefficient KY consists of the product of the incompressible or water coefficient K, and the expansion factor Y. The coefficient K is correlated in the ASME tables by means of the Reynolds number, pipe size, diameter ratio, and pressure-tap location. The value of K, for any one installation, is a function only of the Reynolds number. It decreases with increase in Reynolds numbers up to a certain high value, beyond which K is independent of the viscous forces represented by the Reynolds criterion. Except for very small orifices at low flow rates, the Reynolds number for compressible flow is usually quite large—well beyond the limiting value; as a result, K may be assumed to be a constant. The value of K may be determined by water tests. (The values tabulated in the ASME tables were largely determined by this method.) The value of K may also be established in quite another manner. At low velocities the compressibility effects approach zero, and therefore the flow of a gas through an orifice approaches that of an incompressible fluid. Since the product KY is conveniently linear when plotted versus the orifice-pressure ratio, it is readily extrapolated. The intersection of the KY-curve with the ordinate (at $r = 1.0$) defines the water coefficient K. Values determined in this manner agree well with water flow measurements. [Bean (5) has noted that the effects of compressibility and viscosity are probably interrelated in a complex fashion. But the Reynolds-number effect customarily is confined to K, and the compressibility effects to Y, and this division offers a practical and successful method of data correlation.]

The experimental determinations of the expansion factors (Y) in this work utilized both methods of finding K for the meter. For part (*a*), the meters were installed in strict conformance to ASME specifications, and K values were therefore available. Part (*b*) involved flow in small pipes and the coefficients for the

orifice meter were completely unknown. Therefore the K-coefficients were found by extrapolating the subcritical KY-r curves to unity pressure ratio. The expansion factor Y could then be found by dividing the KY values by K.

Extension of Expansion Factors for Air

Apparatus. Air at pressures up to 100 psi was supplied by a reciprocating-piston compressor (240 cfm) equipped with a five-pass aftercooler. The compressor and auxiliaries were located on the lower level of the laboratory. The two metering orifices, used to measure the mass flow rate, and the test orifice were located on the upper level. The orifices were separated from the air receiver at the compressor by approximately 60 ft of 3-in pipe, thus minimizing pulsations.

Mass Flow. The mass flow rate for each run was measured by two standard orifice meters placed in series with the experimental orifice. The upstream meter was made from (new) 2-in. steel pipe and a pair of commercial orifice flanges (flange taps), while the downstream meter was similar but constructed with 3-in. pipe. Such installation details as the lengths of approach and discharge piping, the location and method of pressure and temperature measurements, and the orifice plate proportions were all determined in accordance with ASME specifications (4). The orifice pressure taps (flange) were duplicated to permit two independent measurements of the orifice pressure differential. The edges of the pressure-tap holes (1/4 in.) were slightly rounded to remove burrs. The initial orifice pressures were measured with single-leg mercury manometers for pressures up to 30 psi; for greater pressures Bourdon-tube test gages, calibrated daily, were used. The pressure differentials across the orifice (maintained between 10 and 50 in.) were measured (in duplicate) by cistern-type water manometers; the value of the pressure differential for each run was taken as the average of the two readings. The temperature of the air stream at each meter was measured, at a location 10 pipe diameters downstream from the orifice, with bare-bulb thermometers held in packing glands. The thermometers were precision-grade with scale divisions of 1/2 deg F. Each meter was equipped with a set of five graduated orifice plates, covering a diameter ratio (β) range of 0.15 to about 0.6. The density of the air was corrected for departures from the perfect-gas relation, and the effect of humidity was taken into account. The coefficients and expansion factors for the orifice meters were taken from ASME tables (6). Analysis shows that the tolerance on the mass flow rate G is of the order of ± 0.9 per cent. The values of G from each meter were averaged to establish the mass flow rate for each test. The agreement between the two meters was used as a criterion in accepting or rejecting a test: If the values differed by more than 1.0 per cent, that particular test was rejected.

Test Orifice Meter. The test meter was made from (new) 2-in. steel pipe and a pair of commercial orifice flanges. The pipe ends were faced flush with the flange faces, and the pipe-flange threaded joints were sweated to ensure airtightness. The straight approach and discharge lengths were 50 and 22 pipe diameters. The meter was modified to include corner taps, throat taps, and pipe taps, as well as the flange taps (4). Corner taps were formed by drilling a 1/8-in. hole at an angle of 45 deg to the orifice plate in the corner formed by the pipe and orifice plate. The gasket between the orifice plate and flange was carefully cut to prevent interference with the pressure-tap holes. The edges of the drilled flange and corner-tap holes were carefully smoothed to remove burrs. Brass (SAE) tubing fittings were inserted into the wall to form the pipe-wall taps (pipe taps and upstream throat taps). The ends of the fittings were filed flush with the inner walls of the pipe, and burrs were removed from the edges of the holes. This method resulted in a tap hole having an inside diameter of about 1/4 in. All pressure connections were made with 5/16-in. copper tubing and (SAE) flared fittings. High-pressure needle valves were installed in the manometer and pressure-gage lines. Each of the four sets of pressure taps was duplicated on opposite sides of the pipe. The pressure-tap lines were valved into four manifolds. Independent pressure measurements were made between each pair of corresponding manifolds.

The value of pressure or pressure differential for each run was taken as the average of the two readings; the method used to measure the pressure differential (Δp) for each run depended upon the pressure ratio. For runs at high pressure ratios, the differential pressure Δp was measured with cistern-type mercury manometers. Low pressure ratios resulted in discharge pressures near atmospheric, and p_2 was measured directly with mercury manometers, having one leg open to the atmosphere. Intermediate pressure ratios necessitated the use of series manometers. Four 50-in. mercury manometers (U-tube) were connected in series, the spaces above the mercury and the connecting tubing being filled with water. Air bubbles were carefully eliminated and each of the two sets of manometers was checked against a single-leg manometer at 30 psi to ensure accuracy. The differential pressure for each run was calculated by summing the displacements of each of the four manometers, making proper allowance, of course, for the water legs. The initial or upstream pressure was measured with a Bourdon-tube test gage which was calibrated for every operating period. The two meters and the test section were tested frequently for air leakage by painting all piping and pressure-tubing joints with soap solution.

The initial temperature of the air stream was measured with a bare-bulb thermometer inserted into the line through a packing gland located 15 pipe diameters upstream from the orifice. The line was not lagged, as the stream temperature never differed from that of the room by more than a few degrees, thus effectively eliminating any error caused by heat transfer through the pipe wall. The orifice plate used in the test meter was made from 1/16-in. stainless-steel plate. It was designed to ASME specifications (7) as regards diameter ratio (β), downstream beveling, etc. The finished diameter d_o was 0.3122 in., resulting in a diameter ratio β of 0.1503. The upstream edge of the orifice plate was formed by making the final boring cut toward the upstream face, and then carefully removing the resultant burr by honing with a fine-grade oilstone held flat against the face of the plate. The result was a square edge that did not reflect light.

Procedure. The compressor was caused to run continuously by controlled bleeding of excess air over that flowing through the meter run. The inlet and discharge pressures at the test section were adjusted to approximately the desired values and then sufficient time was allowed for constant pressures and temperatures to obtain. (The most sensitive indicators of steady flow were the differential water manometers.) When steady flow was established, one operator recorded the pressures and temperatures for the two meters, while a second man recorded the test-section data. If the differential pressures across the standard meters changed during a run, the data were discarded. Little or no difference existed between the pressures at the four upstream tap locations (flange, throat, corner, and pipe); and, since, for a 2-in. pipe, the downstream throat tap and the flange tap coincide, the readings of the throat taps were discontinued.

Range of Variables. One orifice plate ($d_o = 0.3122$ in., $\beta = 0.1503$) was tested with air ($\gamma = 1.40$) over a range of pressure ratios from unity to about 0.13 at nominal upstream pressures of 112, 100, 80, and 60 psia. A majority of the runs were made with the orifice operating at supercritical pressure ratios. Sufficient subcritical runs were made to check the experimental coefficients against the ASME values.

Air Density. The initial density of the air at the orifice was computed from the relation

$$\rho_1 = \frac{p_1 y}{R_m T_1}$$

where y is a correction for departures from the ideal-gas law. The value of y was obtained from the ASME Fluid Meters chart (4), and, in addition, the data of Sage and Lacey (8) were used as a check. (Both sources agreed well in the range encountered in this work.) The gas constant R_m was computed from $R_m = 1545.4/M$, where M is the molecular weight of the mixture of air and water vapor. The air was assumed to be saturated with water vapor at the pressure and temperature in the air receiver. The same value of R_m was used, of course, for density calculation for the two metering orifices and the test orifice.

Experimental Discharge Coefficients (KY). The values of KY were computed for each test from the ASME (4) relationship

$$KY = \frac{G}{0.525\, d_o^2 \sqrt{\rho_1 \Delta p}} \quad \ldots\ldots\ldots\ldots [2]$$

Forty-eight tests on the 0.3122-in. orifice were calculated, and two of these tests were discarded as obviously containing errors. Three values of KY representing corner taps, flange and throat taps, and pipe taps were calculated for each test. The KY-r curve was plotted for each pair of taps. The points were concentrated in narrow bands without exhibiting any differences arising from the initial pressures (112, 110, 80, 60 psia). The best curve that could be drawn for the corner and flange taps consisted of two straight lines, one extending from $r = 1.0$ to $r = 0.63$, and a second line of greater slope extending from $r = 0.63$ to $r = 0.0$. A similar linear correlation resulted for pipe taps; however, the inflection point[4] occurred not at $r = 0.63$ but at $r = 0.77$. *The unity pressure-ratio intercepts* of the KY curves agreed well with the proper K values tabulated (6) by the ASME for flange taps and pipe taps, and with the value of α given by Regeln (9) for corner taps. The limiting value of K for flange taps differed from the Regeln value for corner taps by only 0.2 per cent; accordingly, the value of K for both pairs of taps was taken to be 0.5993, the ASME flange-tap value. The K-value for pipe taps was taken as 0.6068, as listed in the ASME tables.

Expansion Factor Y. Having established and confirmed the three values of K, each experimental value of KY was then divided by the corresponding K to find the expansion factor Y. These values of Y have been plotted versus the orifice pressure ratio r, in Figs. 2 and 3. The corner and flange-tap values form a common curve. The subcritical air data agree well with the (linear) ASME flange-tap and pipe-tap expansion factors. The supercritical data form straight lines which intersect the ASME Y-r lines at $r = 0.63$ for flange (and corner) taps, and at $r = 0.77$ in the case of pipe taps. In Fig. 2 the values of the subcritical expansion factors are best represented by the ASME equation for flange taps (4)

$$Y = 1.0 - (0.41 + 0.35\,\beta^4)\frac{1 - r}{\gamma} \quad \ldots\ldots\ldots [3]$$

At pressure ratios below $r = 0.63$ the air test results for corner and flange taps are represented by the following equation

$$Y = Y_{0.63} - 0.3501\,(0.63 - r) \quad \ldots\ldots\ldots [4]$$

where $Y_{0.63}$ is the value of Y in Equation [3] at $r = 0.63$, and is 0.8916 for air. Correspondingly, the pipe-tap data at high pressure ratios are represented by the following equation (4)

$$Y = 1 - [0.333 + 1.145\,(\beta^2 + 0.7\,\beta^6 + 12\,\beta^{13})]\frac{1 - r}{\gamma} \quad \ldots [5]$$

At pressure ratios below $r = 0.77$, the air test data for pipe taps are represented by

$$Y = Y_{0.77} - 0.364\,(0.77 - r) \quad \ldots\ldots\ldots [6]$$

$Y_{0.77}$ is the value of Y in Equation [5] at $r = 0.77$, and is 0.9410 for air.

Accuracy of Mass Flow Determination. The experimental Y determinations are based upon the use of standard ASME orifice meters to measure the flow rate G. An analysis of the errors affecting the mass flow rate indicates that the probable tolerance on the value of G for each test is ±0.94 per cent. The actual test results showed that an even smaller tolerance might be assigned; the two values of G calculated from the meters for each run agreed surprisingly well. With the exception of a few preliminary tests, every run showed an agreement between the upstream and downstream meter rates within 1.0 per cent. Of the final group of runs, the maximum difference between G, as indicated by the 2-in-diam meter (upstream) and as indicated by the 3-in. meter (downstream), was 0.83 per cent. The average difference was 0.292 per cent (without regard for sign). The meters displayed no consistent differences. For 24 of the 46 runs, the downstream-meter rate was greater than the upstream-meter rate by an average of 0.282 per cent. For the remaining 22 runs, the downstream-meter rate was less than the other meter rate by an average of 0.30 per cent.

Accuracy of Experimentally Determined Y Factors. An analysis of the expansion factors Y, indicates that the tolerance on Y values is about ±1.0 per cent. (The tolerance assigned to Y in the subcritical zone in ASME Fluid Meters (1937) (4) is 0.5 per cent.) This figure applies at a pressure ratio of about 0.5; runs at higher pressure ratios may be expected to be slightly less accurate, the opposite being true at lower pressure ratios.

Extension of Expansion Factors for Steam

To determine the effect of ratio of specific heats γ on the expansion factor Y, essentially the same range of experiments as that made with air ($\gamma = 1.40$) was made using superheated steam ($\gamma = 1.30$). Saturated steam from the laboratory main (140 psi) was passed through a gas-fired superheater. The steam was admitted to the orifice-pipe run through a 2-in. angle valve; and after expansion through the test orifice and a downstream control valve (3-in. steel globe), the steam was discharged into a surface condenser on the lower level of the laboratory. (The steam was desuperheated at the entrance to the condenser by injecting a metered quantity of water.)

Test Orifice Meter. The meter was made from (new) 3-in. seamless-steel pipe and a pair of forged-steel orifice flanges. (Since the air tests had shown similar expansion factor-pressure ratio correlations for flange taps and corner taps, the steam meter was equipped only with flange taps.) The pipe ends were faced flush with the faces of the screwed flanges and the pipe diameter (3.091 in.) at the flanges was determined as the average of eight measurements made with telescoping gage and micrometer. The orifice meter was installed in strict accordance with ASME specifications (7); the straight approach and discharge lengths were 23 and 15 pipe diam. All piping from the superheater to the condenser discharge was lagged with 1 in. of 85 per cent magnesia insulation, and the meter flange was covered with 2 in. of asbestos. The orifice plate, made from 1/4-in. stainless-steel plate, was beveled on the downstream side at an angle of 45 deg, leaving an edge thickness of 1/32 in. The finish-boring cut

[4] This stands in contradiction to Perry's work with pipe taps (10). However, Perry smoothed his data by plotting certain "flow factors" for which he presented equations. Relations for KY as a function of r were based upon these (empirical) equations.

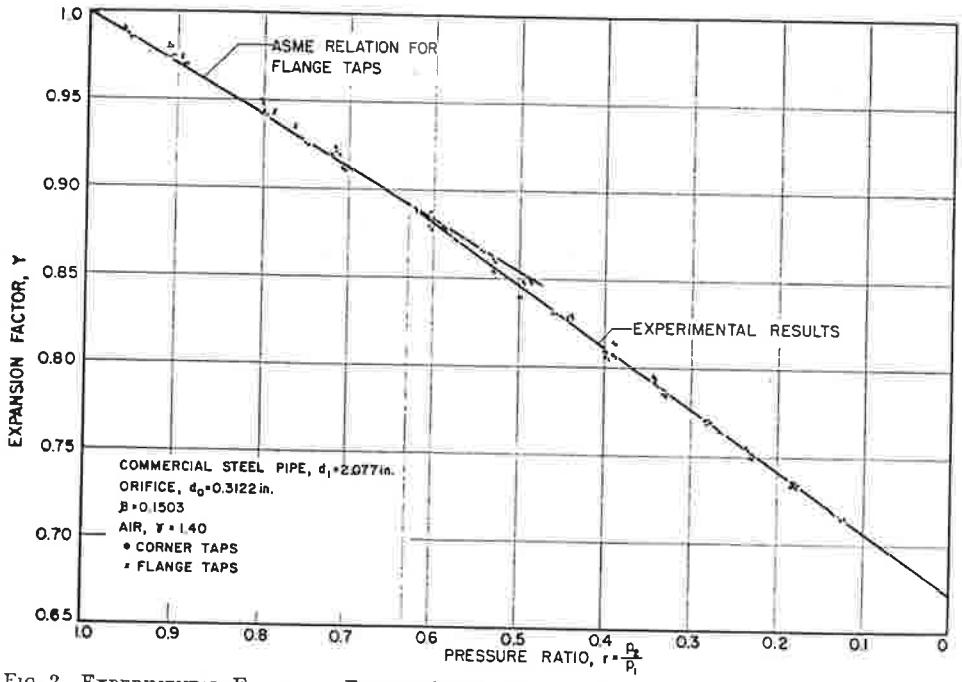

FIG. 2 EXPERIMENTAL EXPANSION FACTORS VERSUS ORIFICE PRESSURE RATIO FOR AIR FLOW IN A 2-IN. PIPE METER (ASME)
(Pressures measured at corner and at flange taps.)

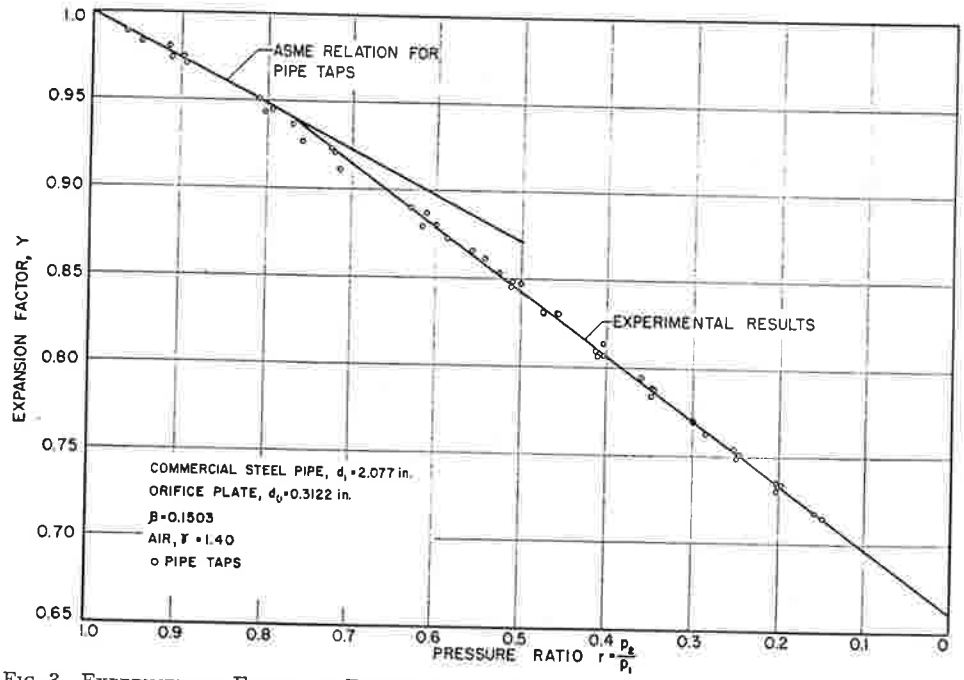

FIG. 3 EXPERIMENTAL EXPANSION FACTORS VERSUS ORIFICE PRESSURE RATIO FOR AIR FLOW IN A 2-IN. PIPE METER (ASME)
(Pressures measured at pipe taps.)

was made toward the upstream face and the burr was carefully removed by honing with a fine oil stone. The finished diameter of the orifice plate was 0.4680 in.; when installed in the 3-in. pipe the diameter ratio was $\beta = 0.1514$. The pressure tap (flange) holes were made with a $^1/_4$-in. drill, and the hole edges were slightly rounded. Both initial and discharge pressures were measured with Bourdon-tube test gages which were calibrated daily. (The taps were not duplicated on opposite sides of the pipe.) An ASME finned thermometer well (11) (stainless steel) was installed at a location 15 pipe diam upstream from the orifice plate. A mercury-in-glass (750 F) thermometer was inserted in the oil-filled well, and the exposed end of the well was insulated to reduce heat transfer. Stem-temperature readings (measured by fastening a mercury thermometer to the exposed stem) were recorded and stem corrections were applied to the steam thermometer readings.

Test Procedure. About 3 hr were required to establish equilibrium values of pressure and temperature at the orifice meter. It was possible to maintain a constant initial pressure at the orifice by occasional adjustment of the inlet (angle) control valve. The steam temperature was controlled by adjusting the firing rate of the superheater; however, variations of 3 to 4 F did occur during a test. The temperature was recorded every 2 min during the 35-min tests, and these readings were averaged to find the run temperature. After steady flow was established at the desired pressure and pressure ratio, the condensate and injection water tanks were weighed and two stop watches were started. Frequent short checks were made of the flow rate at the condensate tank to detect rate changes during a run (the condenser was operated at atmospheric pressure). The water tanks were weighed again (simultaneously) at the end of a run.

Range of Variables. One orifice plate (d_o = 0.4680 inch, β = 0.1514) was tested with steam at pressure ratios down to r = 0.127 with flange taps. The runs were made in four groups with constant initial pressures of 113, 92, 75, and 60 psia and with a constant superheat of about 100 F.

Experimental Discharge Coefficients. The values of KY were computed for fifty tests from the relationship

$$KY = \frac{G_s}{0.525\, E d_o^2 \sqrt{\rho_1 \Delta p}} \quad \ldots\ldots\ldots\ldots [7]$$

where E is a factor to compensate for the area enlargement of the orifice from thermal expansion (7). At any one initial pressure, the average steam temperature t_1 varied by less than 10 F; hence it was assumed that the steam density would respond to the small temperature variations as an ideal gas, and the mass flow rate for each test was corrected for the deviation of the run temperature from a selected average value t_s. The relation is

$$G_s = G \sqrt{T_1/T_s}$$

where G and T_1 are the actual test values and T_s is the mean temperature for the particular group of tests. Having thus adjusted the mass flow rates, the initial density was taken from steam tables (12) at the constant pressure (p_1) and mean temperature (t_s) for each of the four groups of tests.

The individual KY-values were plotted versus the orifice-pressure ratio. Despite the wide scatter of the data (when compared to the tests on air), the ordinate intercept (at r = 1.0) of the KY-curve agreed well with the high Reynolds number ASME value: K = 0.5952.

Expansion Factors Y. The Y values (KY divided by 0.5952) are plotted versus the orifice pressure ratio in Fig. 4. The ASME expression (Equation [3]) for Y (γ = 1.3) is plotted as the solid line in the subcritical region; a second straight line is drawn to represent the supercritical data. Note that the supercritical line intersects the ASME curve at r = 0.63. It will be recalled that similar results were obtained with air, but the slope increase at r = 0.63 is only about one half that for air. (The change in γ from 1.4 to 1.3 no doubt affects this inflection pressure ratio, but the [steam] data are insufficient to show the nature of the effect.)

The supercritical data for steam are represented by the relation

$$Y = Y_{0.63} - 0.3480\,(0.63 - r) \quad \ldots\ldots\ldots\ldots [8]$$

where $Y_{0.63}$ is the value calculated from Equation [3] for r = 0.63, and is 0.8833 for γ = 1.3. (Equation [8], probably, also applies to corner taps at low diameter ratios, since the air tests established the identity of the flange-tap and corner-tap Y-r correlations, at β = 0.15.)

Accuracy of Experimental Y Curve. A mathematical analysis of the errors affecting Y indicates the tolerance to be slightly over ±1.0 per cent. However, examination of Fig. 4 shows that the spread of experimental data, even in the supercritical region, is of the order of ±3.0 per cent, a scatter that is quite inferior to the results obtained with air. For some reason, the computed Y-values for the 113- and 92-psia tests fell below the values for the 75 and 60-psia tests. This apparent pressure effect accounts, in part, for the wide scatter of data. Such a pressure effect is

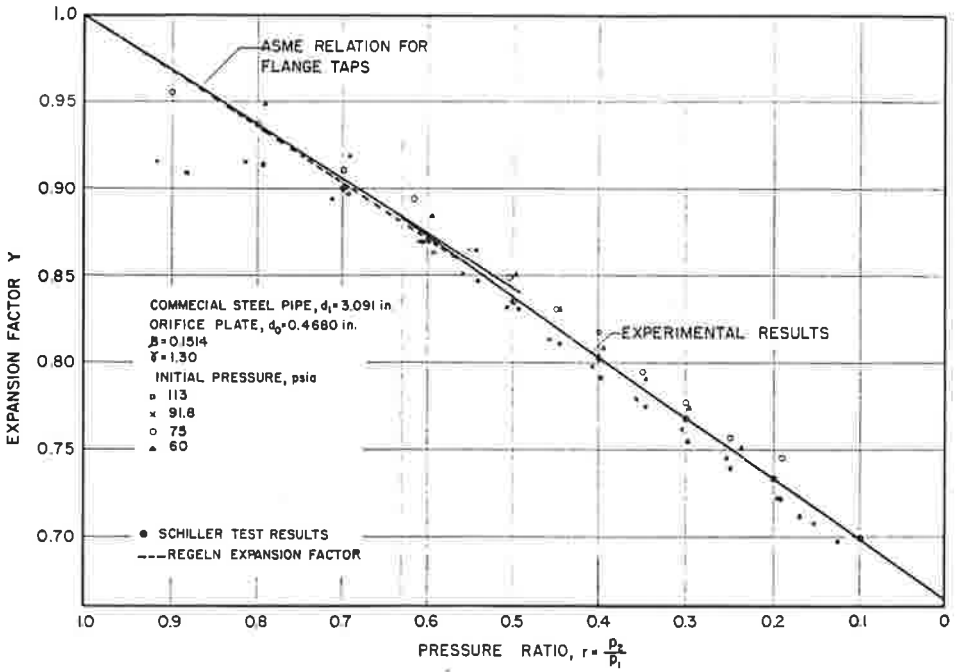

FIG. 4 EXPANSION FACTORS MEASURED FOR FLOW OF SUPERHEATED STEAM IN A 3-IN. PIPE METER
(Standard ASME orifice meter, using flange taps.)

not to be expected and probably stems from a systematic error in the experimental technique.

Comparison With Other Data. Although Schiller's (13) data for steam were taken with German standard orifices (corner taps), they may be compared with the present results, since the air tests have established that the Y-r curves for flange taps and corner taps are identical (for $\beta = 0.15$ only). Values of Y have been calculated from Schiller's data for $\beta = 0.2$ and are plotted, for comparison, in Fig. 4. In addition, a dotted line has been drawn in the subcritical region to represent the Regeln values for the expansion factor, (for steam, $\gamma = 1.31$). The agreement of Schiller's data and the Regeln curve with the experimental results is evident.

Maximum Mass Flow Rate. A few investigations of compressible flow through orifices (1, 14, 15) have indicated maximum flow ratios of the order of 0.2, i.e., further reduction in the discharge pressure had no effect on the flow rate. This group of tests, conducted at pressure ratios as low as 0.13 for both air and steam, showed that the flow rates continued to increase as the discharge pressure was lowered. A few tests were made with steam at pressure ratios down to 0.074, with no apparent limiting flow being reached. Rateau (16) and Reynolds (17) obtained data at ratios as low as $r = 0.04$ and 0.10, respectively, with similar results.

Supercritical Flow With High Velocities of Approach

For diameter ratios greater than about 0.4, the approach or pipe-line velocity becomes an appreciable factor. The approach velocity is directly proportional to the flow rate and hence varies with the orifice pressure ratio. The combination of a large diameter ratio β and a low orifice pressure ratio creates two unique problems:

1 Violent shock discontinuities exist in the orifice jet. These disturbances logically might be expected to complicate measurement of the discharge pressure when the pipe wall is in close proximity to the jet.

2 The stream temperature can no longer be measured in the usual manner, because stagnation of the high-velocity fluid on the thermometer causes a temperature to be indicated that is higher than the actual static stream temperature.

The investigations of Hodgson (19) and Schiller (13) appear to be the only two sources of data on supercritical flow at high β values in the literature.[5] They are alike in two important respects: (*a*) both used corner taps to measure the orifice-meter pressures, and (*b*) both apparently neglected the fact that temperature measurement constituted a special problem.

To investigate the flow characteristics with a square-edged orifice and a high approach velocity, the 2-in. pipe test section used for air was replaced with a small ($d_1 = 0.527$ in.) pipe and orifice flanges. Orifice plates ranging from $\beta = 0.2$ to $\beta = 0.8$ were tested in the small pipe over a wide range of pressure ratios.

High-Velocity Test Section. The general arrangement of the test section and details of the orifice meter are shown in Fig. 5. The meter was made from $^5/_8$-in. (hard) drawn copper tubing ($d_1 = 0.527$ in.) and a pair of orifice flanges machined from brass. The two flanges were sweated onto the tubing and the final facing operations were made with the tubing held in a lathe collet, thus ensuring that the recesses cut in the flange faces would be concentric with the tubing. The corner taps were drilled at an angle of 45 deg to the flange faces as shown in Fig. 5. In addition, another set of taps was located in the pipe wall, 1 pipe diam above and 1 diam below the upstream face of the orifice plate. These taps will be referred to as "wall taps" in the following section. In addition, a third downstream tap was located

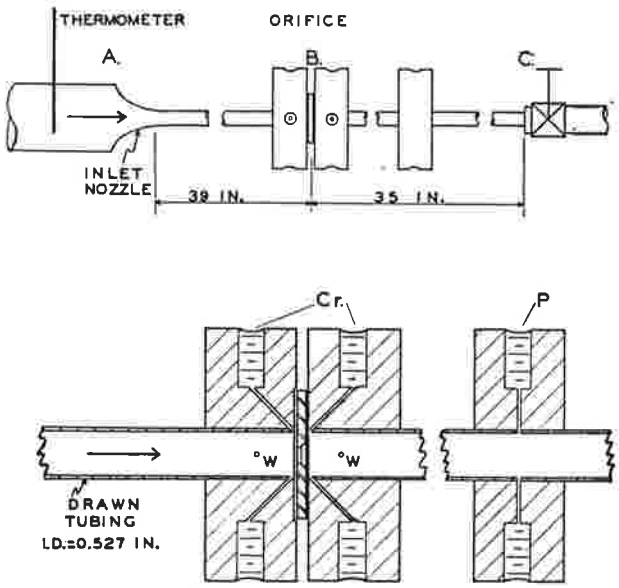

Fig. 5 Orifice Meter Used for Air-Flow Tests With High Approach Velocities

(Cr: corner taps; W: wall taps, 1 diam upstream and downstream from face of orifice plate; P: pipe tap, 8 pipe diam downstream from face of orifice plate.)

8 diam from the orifice plate in the standard pipe tap location. Thus pressures could be measured at the following:

1 Corner taps.
2 Wall taps, located 1 diam from the face of the orifice plate.
3 A downstream pipe tap, 8 diam from the orifice plate.

The taps were duplicated on opposite sides of the pipe, and all (ten) of the tap holes were drilled with a No. 60 drill (0.040 in.). The bore of the tube was polished with crocus cloth to remove burrs. The method of pressure measurement (by manifolding the lines) was similar to that described for the 2-in. pipe meter, the only difference being that the pressure differential, for the intermediate range of orifice-pressure ratios, was determined by measuring the discharge pressures directly with a gage.

The entry to the test section (at A, Fig. 5) consisted of a polished convergent nozzle having a throat diameter equal to that of the tubing inside diameter. The inlet end of the nozzle (2 in. diam) was coupled to the 2-in. discharge pipe from the upstream metering orifice. The approach (A–B) of the test meter was long in length to ensure uniform flow at the orifice. The discharge length (B–C) terminated in a $1^1/_2$ in. globe valve which was used to regulate the downstream pressure. The air was finally discharged to the atmosphere through the downstream metering orifice. All piping joints and pressure tap lines, from the upstream meter inlet to the downstream meter outlet, were checked frequently for leaks (with soap solution). The initial pressures at the test orifice, as well as the discharge pressures at pressure ratios near 0.5, were measured with a precision dial manometer. For the range encountered, the gage could be read to about $^1/_{10}$ per cent accuracy; it was specially calibrated by the manufacturer and checks in the laboratory indicated that

[5] At least with data based upon initial static pressure and temperature. Grey and Wilsted (20) and Neal (10) have presented adiabatic discharge coefficients based upon total pressure and total temperature. Except for very small diameter ratios, the two forms are not directly comparable. Through continuity, total head coefficients may be converted to the usual form, but the relations are rather complex.

for the range in which it was used, no corrections were necessary.

Temperature Measurement. In addition to the fact that high fluid velocities produce thermometer errors, the tube size (0.527 in.) was such that a thermometer or thermocouple inserted through the tube wall would seriously restrict and disturb the flow. As an alternative, the temperature of the air was measured in the 2-in. pipe a few diameters upstream from the convergent entry nozzle (at A in Fig. 5). The assumption was made that the air upstream from the nozzle possessed zero velocity—a valid assumption, since the maximum velocity in the 2-in. pipe for any of the tests was less than 40 ft/sec. The flow from the nozzle entry to the orifice was assumed to be adiabatic because:

1 The stream temperature (t_i) in the 2-in. pipe was essentially equal to the temperature of the room.

2 Frössel used a similar nozzle and tube arrangement in his determinations of high-velocity friction factors. Frössel found that ". . . . as a result of friction, the gas in the neighborhood of the wall acquired approximately the temperature of the outside air so that no heat exchange takes place through the pipe wall" (21).

By thus assuming the total energy of the flow to be constant, the total temperature at the orifice is equal to the (total) temperature at the tube nozzle entrance, and the stream temperature t_1 at the orifice may be calculated.

The enthalpy before (h_i) and after (h_1) expansion in the entry nozzle are related by

$$h_i = h_1 + \frac{w_1^2}{2g_c} \quad \ldots\ldots\ldots\ldots\ldots\ldots [9]$$

Since air can be assumed to be an ideal gas, then $h = C_pT$ and $pv = RT$. These relationships along with the continuity equation $G = \rho_1 w_1 A_1$ can be substituted into Equation [9]

$$T_1^2 + \left[\frac{2g_c A_1^2 C_p}{R^2}\left(\frac{p_1}{G}\right)^2\right] T_1 - \left[\frac{2g_c A_1^2 C_p}{R^2}\left(\frac{p_1}{G}\right)^2\right] T_i = 0$$

$$\ldots\ldots\ldots\ldots\ldots\ldots\ldots\ldots [10]$$

and thus the static temperature T_1 is a function of the known quantities T_i, p_1, and G. Equation [10] was used to compute the stream temperature T_1 for runs with high approach velocities. In the majority of the tests, the difference between T_1 and T_i was small; however, the difference was appreciable for tests on orifices with diameter ratios of 0.7 and 0.8.

Prediction of Stagnation Error. By continuity and the ideal gas relation

$$w_1 = \frac{G}{A_1\rho_1} = KYm\sqrt{1-r}\ \sqrt{2g_cRT_1} \ldots\ldots [11]$$

By combining Equation [11] with the isentropic velocity equation

$$w_1 = \sqrt{\frac{2g_c\gamma}{\gamma-1}RT_i\,[1 - T_1/T_i]} \ldots\ldots\ldots [12]$$

it follows that

$$(KY)^2 m^2 (1-r) = \frac{\gamma}{\gamma-1}[T_i/T_1 - 1] \ldots\ldots [13]$$

From Equation [13] the ratio of the total temperature T_i to the static stream temperature T_1 may be calculated at any pressure ratio on the basis of the KY-value.

Orifice Plates. The square-edged orifice plates, machined from $^1/_{16}$-in. carbon steel, were 1.48 in. diam. The downstream faces of the plates were beveled at an angle of 45 deg. Dimensional details are given in Table 1.

TABLE 1 DIMENSIONS OF ORIFICE PLATES

Nominal β	d_o, in.	Edge-width ratio, L/d_o	$\beta = \frac{d_o}{0.527}$
0.2	0.10724	0.1090	0.2035
0.3	0.15953	0.0805	0.3027
0.4	0.21327	0.0284	0.4047
0.5	0.26547	0.0413	0.5037
0.6	0.32248	0.0226	0.6119
0.7	0.37150	0.0220	0.7049
0.8	0.42535	0.0263	0.8071

The dimensions were determined by measurements with a cathetometer microscope. The values of d_o for each plate were established as the average of 8 measurements across 4 diam. Previous investigations have shown that the thickness of the orifice plate does not affect the discharge characteristics providing the edge-width ratio L/d_o is small. The ASME specification (7) in this respect is $L/d_o \leq 0.125$; thus all of the plates conform.

Test Procedure. The tests were conducted in the manner previously described for the 2-in. pipe meter. The mass flow rate G was similarly measured with two standard meters. Duplicate readings of the pressure differentials were not recorded; rather, checks were made with each orifice plate installed to ensure that the pressures at the taps on one side of the line agreed with those of the diametrically opposite taps. No differences were detected for any of the orifice plates.

Range of Variables. Seven orifice plates, representing a range of diameter ratios of 0.2 to 0.8, were tested at a nominal initial pressure and temperature of 90 psia and 75 F over a range of pressure ratios from unity to about 0.14. The orifice-meter pressures were measured at two pairs of taps and at a downstream pipe tap for each test.

Experimental Discharge Coefficients KY. Discharge coefficients were computed for each of an original group of 149 tests. Of this number, four tests were discarded as obviously in error. The calculations were based upon a discharge pressure measured at the corner tap (p_{2c}) and on an upstream pressure measured at the wall tap (p_{1w}) located 1 pipe diam upstream from the orifice. The corner-tap initial pressure p_{1c} is nearly equal to p_{1w} for flow through orifice plates of low diameter ratios (and for all flows near unity pressure ratio). Whenever the approach velocity becomes appreciable, a ram effect occurs at the face of the orifice, and the corner-tap pressure is increased: $p_{1c} > p_{1w}$. It was decided to base the calculations on p_{1w} and p_{2c} for the following reasons:

1 Calculation of the density ρ_1 in the ASME equation requires knowledge of p_1, the static stream pressure. The corner pressure p_{1c} represents the static pressure plus some unknown ram effect.

2 The method of forming the corner taps was, of necessity, arbitrary. Although the downstream (p_{2c}) reading may reasonably be expected to be unaffected by high-velocity phenomena, the "recovery factor" of the upstream taphole is an unknown quantity. On the other hand, the simple wall-pressure measurement is dependable and easily reproduced; it may be relied upon as a close approximation to the "true" static pressure.

3 The method is not unprecedented. Witte reported data on a similar basis (22).

The KY-coefficients are plotted versus the orifice pressure ratio p_{2c}/p_{1w} in Fig. 6. Individual plots of the data for $\beta = 0.2$, 0.3, 0.4 revealed that the data were all essentially alike; accordingly, the test values for all three of the low-diameter-ratio plates were plotted to form one curve in Fig. 6. Separate curves are shown for the remaining four orifices. All of the coefficients

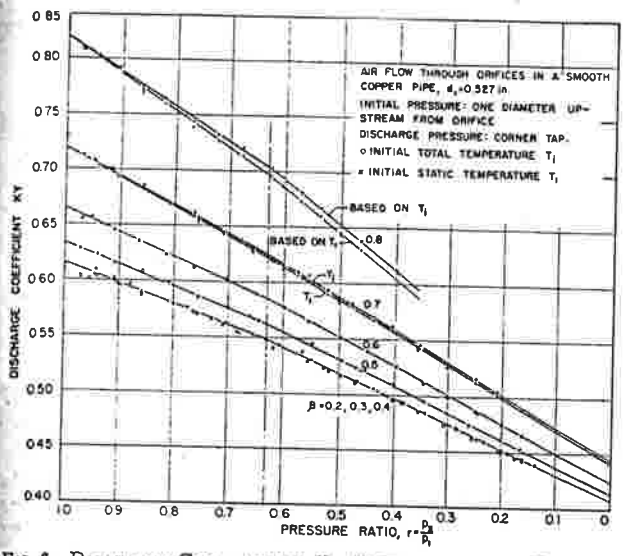

FIG. 6 DISCHARGE COEFFICIENTS KY DETERMINED FROM TESTS ON SEVEN ORIFICE PLATES IN A SMOOTH COPPER PIPE

were calculated originally on the basis of T_i, the total temperature. Where warranted, the coefficients were recomputed on the basis of T_1 (as established by Equation [10]). The differences between T_i and T_1 were negligible for the five smallest plates, i.e., $\beta = 0.2$ to 0.6. (The value of $T_i - T_1$ was a maximum of about 4 deg for $\beta = 0.6$.) However, all of the runs on the two largest plates were computed on the basis of T_1 as well as T_i. The maximum temperature differentials occurred for the low-pressure-ratio tests on the $\beta = 0.8$ plate, and were of the order of 10 to 15 deg. Two KY-r curves, based on T_i and T_1 have been drawn for the $\beta = 0.7$ and 0.8 plates; the progressive separation of the coefficient curves illustrates the temperature effect. At a pressure ratio of $r = 0.5$, the difference between the coefficient curve, based upon the total temperature T_i and the curve based upon T_1, amounts to about 0.6 per cent for $\beta = 0.7$ and 1.25 per cent for $\beta = 0.8$.

The graphical presentation of the coefficients in Fig. 6 reveals some interesting facts:

1 The subcritical KY-data form a linear relation from $r = 1.0$ to $r = 0.63$.

2 A second straight line represents the data from $r = 0.63$ to the limit of the test-pressure ratios.

3 A change of flow regime apparently occurs at $r = 0.63$ for all of the diameter ratios.

It will be recalled that similar results were obtained with the air data and with the steam data, ($\beta = 0.15$).

Determinations of K by Extrapolation. Since no established water coefficients exist for a meter as small as 0.527 in. diam, the values of K for each orifice plate were determined by extrapolating the (subcritical) KY-r curve to $r = 1.0$. The resultant values are given in Table 2, along with the KY-values at $r = 0.63$ and $r = 0.0$.

The values of K for diameter ratios up to 0.7 are represented to within 1.3 per cent by the relation

$$K = 0.608 + 0.415\,\beta^4 \quad \ldots\ldots\ldots\ldots\ldots [14]$$

This equation for K is included to emphasize the conventional behavior of K as a function of β, despite the very small diameter of the orifice meter.

Expansion Factor Y Versus Pressure Ratio. The data in Table 2 are sufficient to establish the expansion-factor curves for the seven orifice plates; the KY-values at $r = 0.63$ and $r = 0$ were divided by K for each orifice plate; the value of Y at $r = 1.0$ is, of course, unity. The Y-r relations appear in Fig. 7.

TABLE 2 EXPERIMENTAL DISCHARGE COEFFICIENTS FOR AN ORIFICE METER WITH HIGH VELOCITIES OF APPROACH

Nominal β	K (KY at $r = 1.0$)	KY at $r = 0.63$	KY at $r = 0.0$
0.2	0.616	0.548	0.407
0.3	0.616	0.548	0.407
0.4	0.616	0.548	0.407
0.5	0.634	0.562	0.413
0.6	0.665	0.585	0.423
0.7	0.719	0.624/0.622[a]	0.445/0.440[a]
0.8	0.820	0.703/0.696[a]	0.452/0.444[a]

[a] The two values are, respectively, KY for T_i and KY for T_1.

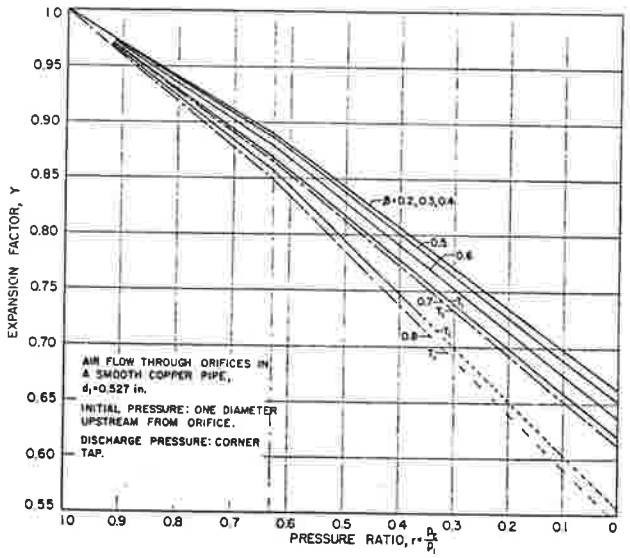

FIG. 7 EXPANSION FACTORS FOR AIR FLOW THROUGH AN ORIFICE METER AT LOW PRESSURE RATIOS FOR DIAMETER RATIOS FROM 0.2 TO 0.8

The value of the expansion factor is little affected by minor changes in pressure-tap location near the orifice plate. The ASME (subcritical) relation (4) for Y is linear, as is ϵ, the "Regeln" (9) expansion factor. In Table 3 the values of the experimental Y-values at $r = 0.63$ are compared with the values computed from the ASME equation

$$Y = 1 - (0.41 + 0.35\,\beta^4)\frac{1-r}{\gamma} \quad \ldots\ldots\ldots\ldots [3]$$

for flange taps, and with the values of ϵ at $r = 0.63$ taken from Regeln for corner taps.

TABLE 3 EXPANSION-FACTOR VALUES AT $r = 0.63$, $\gamma = 1.40$

β	Regeln ϵ	ASME Y	Experimental Y
0.2035	0.889	0.8915	0.890
0.3027	0.889	0.8909	0.890
0.4047	0.887	0.8892	0.890
0.5037	0.883	0.8857	0.886
0.6119	0.875	0.8787	0.879
0.7049	0.863	0.8689	0.868/0.865[a]
0.8071	0.845	0.8524	0.857/0.849[a]

[a] The two values are, respectively, Y for T_i, and Y for T_1.

The experimental values for Y agree well with the ASME values; the Regeln values are lower by about 0.3 per cent at small values of β, to about 0.8 per cent at large values of β.

Considering this agreement (Table 3) of subcritical Y-values, it is probable that supercritical flow through standard (large)

meters can be predicted on the basis of the results demonstrated in Fig. 7.

At pressure ratios below 0.63, the expansion factor for $\beta = 0.2$, 0.3, 0.4 is represented by the following relation

$$Y = Y_{0.63} - 0.365\ (0.63 - r) \quad [15]$$

where $Y_{0.63}$ is the value from Equation [3] at $r = 0.63$ for the proper diameter ratio. Supercritical data for the larger plates may be represented by similar equations. (The slope increase in the Y-r curves, at $r = 0.63$, is less for the larger orifice plates.)

Significance of Y-r Inflection Point. The correlation of Y with pressure ratio demonstrates that compressible flow in an orifice undergoes fundamental change in flow regime at, or near, $r = 0.63$. It is reasonable to assume that high-velocity compressibility effects account for the different Y-r correlations at low and at high pressure ratios. Local accelerations in the flow afford a logical explanation for the fact that the inflection occurs not at $r = 0.528$, the theoretical critical ratio, but at $r = 0.63$. Stream filaments adjacent to the orifice plate undergo large accelerations, and, no doubt, sonic velocities are encountered at the edge of the plate before the over-all pressure ratio is sufficiently low to produce (one-dimensional) sonic velocity.

Summary of Expansion Factors. Air and steam flow measurements at $\beta = 0.15$, and air flow at high approach velocities, all produced Y-r correlations that had inflection points at $r = 0.63$, when based upon pressure taps located close to the orifice plate. (While it is likely that the inflection points were affected by the specific-heat ratio γ, and the diameter ratio β, the amount of data did not warrant investigation of these variables. The net effect on the pressure ratio of the inflection would be quite small.)

The agreement of the subcritical experimental data with the ASME expression for Y suggests that the ASME (4) equation

$$Y = 1 - (0.41 + 0.35\,\beta^4)\frac{1 - r}{\gamma} \quad [3]$$

be modified as a means of establishing an equation to represent Y at low pressure ratios. On this basis, the results of air-flow tests in a 2-in. pipe meter (flange and corner taps $\beta = 0.15$, Fig. 2), may be represented by

$$Y = Y_{0.63} - 0.3501\ (0.63 - r) \quad [4]$$

where $Y_{0.63}$ is Y from Equation [3] at $r = 0.63$.

Similarly, for superheated steam ($\gamma = 1.3$, $\beta = 0.15$, $d_1 = 3$ in., Fig. 4)

$$Y = Y_{0.63} - 0.3480\ (0.63 - r) \quad [8]$$

The expansion-factor data for the high velocity of approach tests (for $\beta = 0.2$ to 0.4, Fig. 7) may be represented by

$$Y = Y_{0.63} - 0.365\ (0.63 - r) \quad [15]$$

Similar equations may, of course, be written for the other expansion-factor curves in Fig. 7. It is noted that the increase in slope of the Y-r lines at $r = 0.63$ is less for large than for small values of β.

The diameter ratio β has little effect, when small, on the expansion factor Y. Consequently, Equations [4] and [8] for the 2-in. and 3-in. meters (at $\beta = 0.15$) are probably applicable to diameter ratios as large as 0.4.

Theoretical Experimental Comparisons

Chaplygin (23) in 1904, presented an analytical solution for the subcritical efflux of a gas from a slit in a plane wall; and the period of 1930 to 1933 marked the appearance of several (24, 25, 26, 27, 28, 29) approximate theoretical solutions to the problem of subcritical compressible flow through orifices. Although a few of these solutions have been extrapolated (erroneously) to supercritical pressure ratios (13, 23, 27), no successful means of predicting the flow behavior of an orifice at very low pressure ratios has been known. In conjunction with the present investigation an equation was derived (18) that predicts the contraction behavior of the gas jet at supercritical pressure ratios. The contraction coefficient, in conjunction with certain one-dimensional gas-dynamics relations, renders possible the prediction of the mass flow rate for a square-edged orifice. This new solution, plus the solution of Buckingham (27) for the subcritical zone, enables the gas flow rate of an orifice meter to be predicted quite accurately over the entire range of pressure ratios from unity to zero. In common with other approximate theoretical solutions, the gas jet-contraction coefficient was established by correcting the incompressible or water coefficient for the effects of compressibility. Impulse-momentum relations[6] were applied to the orifice jet at the minimum section of the convergent-divergent stream where the jet pressure and velocity are constant and of critical magnitude.

The supercritical contraction coefficient μ_g, which represents the ratio of the minimum or critical jet area to the area of the orifice, was expressed in the form of a cubic equation

$$\mu_g^3\,[r_c^{2/\gamma}\,m^2\,(r_c - r)] + \mu_g^2\,[r_c^{2/\gamma}]\left[\frac{\gamma}{\gamma - 1}\left(1 - r_c^{\frac{\gamma-1}{\gamma}}\right)\left(m^2 + \frac{2}{\mu} - \frac{1}{\mu^2}\right) - m^2(1 - r)\right] - \mu_g\left[\frac{2\gamma}{\gamma - 1}\,r_c^{1/\gamma}\left(1 - r_c^{\frac{\gamma-1}{\gamma}}\right) + (r_c - r)\right] + [1 - r] = 0 \quad [16]$$

Equation [16] demonstrates that the jet contraction[7] μ_g is dependent upon the pressure ratio r, the ratio of specific heats γ, the orifice-pipe area ratio m, the incompressible contraction coefficient μ, and the critical pressure ratio r_c. The term r_c was shown to be related to m and γ by the following equation

$$r_c^{\frac{1-\gamma}{\gamma}} + \frac{\gamma - 1}{2}\,\mu_g^2\,m^2\,r_c^{2/\gamma} = \frac{\gamma + 1}{2} \quad [19]$$

---

[6] Unlike the Borda nozzle, the pressure on the upstream face of the orifice plate is not uniform, but diminishes near the edge of the opening. To overcome this problem, resort was made to a relation devised by Buckingham (27) in his approximate theoretical solution for the subcritical case: The force exerted on the upstream face of the orifice plate by a compressible fluid and by an incompressible fluid are equal under certain conditions. The validity of the method is evidenced by the excellent agreement between experimental (subcritical) data and Buckingham's solution.

[7] Compressible flow in a Borda nozzle was similarly treated, and the following expression for the supercritical contraction coefficient was derived

$$\mu_g = \left.\frac{1 - r}{r_c(\gamma + 1) - r}\right|_{r \geqslant r_c} \quad [17]$$

As was the case with the orifice solution, this expression may be solved at $r = 0$, yielding a value of $\mu_g = 0.790$ for $\gamma = 1.40$. The subcritical contraction coefficient was previously established by Busemann (30)

$$\mu_g = \frac{\gamma - 1}{2\gamma}\left[\frac{1 - r}{r^{1/\gamma} - r}\right]_{r \geqslant r_c} \quad [18]$$

The two equations are identical at the critical pressure ratio.

If the velocity of approach is zero

$$r_c = \left(\frac{2}{\gamma + 1}\right)^{\frac{\gamma}{\gamma - 1}} \quad \ldots\ldots\ldots\ldots\ldots\ldots [20]$$

Once m, the area ratio for the orifice meter, is selected, the value of μ is established, i.e., it is the incompressible flow coefficient for that orifice, at high Reynolds numbers.

The mass flow rate, at supercritical pressure ratios, may be found from

$$G = \mu_g m A_1 \sqrt{\frac{2g_c\gamma}{\gamma - 1} p_1 \rho_1 \left[\frac{\left(r_c^{2/\gamma} - r_c^{\frac{\gamma+1}{\gamma}}\right)}{1 - \mu_g^2 m^2 r_c^{2/\gamma}}\right]} \quad \ldots\ldots [21]$$

and the value of μ_g from Equation [16]. Buckingham (27) derived an expression for μ_g for the case of subcritical flow. His quadratic-equation solution may be expressed, in the nomenclature of this paper, as

$$\mu_g = \frac{Z}{r^{1/\gamma} B}\left[1 - \sqrt{1 - \frac{B r^{2/\gamma}}{Z^2}}\right] \quad \ldots\ldots\ldots [22]$$

where

$$Z = \frac{\gamma}{\gamma - 1}\left[\frac{r^{2/\gamma} - r^{\frac{\gamma+1}{\gamma}}}{1 - r}\right]$$

$$B = Z\left[m^2 + \frac{2}{\mu} - \frac{1}{\mu^2}\right] - m^2 r^{2/\gamma}$$

Using μ_g from Equation [22], the mass flow may be found from

$$G = \mu_g m A_1 \sqrt{\frac{2g_c\gamma}{\gamma - 1} p_1 \rho_1 \left[\frac{r^{2/\gamma} - r^{\frac{\gamma+1}{\gamma}}}{1 - \mu_g^2 m^2 r^{2/\gamma}}\right]} \quad \ldots\ldots [23]$$

At the critical pressure ratio, the supercritical Equation [16] for μ_g reduces to identity with the subcritical Equation [22]. The supercritical solution for μ_g and Buckingham's subcritical solution were compared with the experimental results of Bachmann (31) for air flow, and with Schiller's data (13) on superheated steam. The theoretical solutions predicted the experimental results to within 1 per cent; the difference increased to 2 per cent at pressure ratios below 0.2.

By eliminating the mass flow rate G between the ASME equation and the isentropic equation, a relation can be obtained in which a theoretical expansion factor Y_{th} is expressed as a function of the theoretical coefficient μ_g. The relationship is

$$Y_{th} = \frac{\sqrt{\frac{\gamma}{\gamma - 1}\left(r^{2/\gamma} - r^{\frac{\gamma+1}{\gamma}}\right)}}{K\sqrt{1/\mu_g^2 - m^2 r^{2/\gamma}}\sqrt{1 - r}} \quad \ldots\ldots\ldots [24]$$

for the subcritical case where μ_g is computed from Buckingham's Equation [22] and

$$Y_{th} = \frac{\sqrt{\frac{\gamma}{\gamma - 1}\left(r_c^{2/\gamma} - r_c^{\frac{\gamma+1}{\gamma}}\right)}}{K\sqrt{1/\mu_g^2 - m^2 r_c^{2/\gamma}}\sqrt{1 - r}} \quad \ldots\ldots\ldots [25]$$

for the supercritical range of pressure ratios where the value of μ_g is computed from the cubic Equation [16].

The information necessary to establish μ_g is m, μ, r, and r_c. The incompressible, or liquid, contraction coefficient μ may be found from the water coefficient K by the relationship

$$\mu = \frac{K}{\sqrt{1 + m^2 K^2}} \quad \ldots\ldots\ldots\ldots\ldots [26]$$

The theoretical Y-r curves from $r = 1.0$ to $r = 0$ have been plotted for two of the orifices tested:

1 The (ASME) 2-in. pipe meter with $\beta = 0.15$, $\gamma = 1.40$,
2 The mid-range orifice plate of the series tested in the 0.527, in. line: $\beta = 0.5$, $\gamma = 1.40$.

Note that for 1, K was taken from the ASME tables, and for 2, K was obtained by extrapolation of the KY-r curve to $r = 1.0$.

In Figs. 8 and 9 the solid-line curves represent the theoretical solution, and the points represent the individual Y-values determined by experiment. The comparison shows that the theoretical solution predicts experimental results to within 1 per cent over most of the range of pressure ratios, the difference increasing to a maximum of 2 per cent at $r = 0.12$ for the 2-in., $\beta = 0.15$, meter. Thus the correlations obtained with the data of Bach mann and Schiller have been confirmed by new experimental evidence.

Summary

Experimental Results. Probe investigation of air and steam jets showed that (*a*) Stanton's findings are applicable to an orifice with unrestricted approach, (*b*) shock disturbances first occur at or near the critical pressure ratio and are present for all lower ratios, and (*c*) apparently no shock disturbances exist at the edge of the orifice, the initial shock occurring downstream in the free jet.

The discharge coefficients for the flow of air (2-in. pipe meter) and for the flow of steam (3-in. pipe meter) were measured at pressure ratios from unity to 0.13. The diameter ratio β of both meters was 0.15. Steam flow tests at pressure ratios as low as $r = 0.074$ (and for air, $r = 0.13$) failed to detect a limiting mass flow rate (as previously reported by some investigators). For the air tests, the orifice-meter pressures were measured at duplicate flange, corner, throat, and pipe taps. Values of the expansion factor Y were computed for each air test and plotted versus the orifice-pressure ratio; the corner and flange-tap values formed a common curve. The subcritical air data agreed well with the (linear) ASME flange-tap and pipe-tap expansion-factor equations. The supercritical data formed straight lines which intersected the ASME (Y-r) lines at $r = 0.63$ for flange (and corner) taps, and at $r = 0.77$ in the case of pipe taps.

Similar results were obtained with the experimental flange-tap data for steam. Again, the subcritical data were best represented by the ASME expansion-factor equation. The supercritical data formed a straight line which intersected the ASME curve at $r = 0.63$; the change in slope at this ratio was considerably less for the steam data ($\gamma = 1.3$) than for the air data ($\gamma = 1.4$).

The effects of high approach velocity were investigated by measuring discharge coefficients (KY) for the flow of air through orifices in a 0.527-in. smooth pipe with diameter ratios from 0.2 to 0.8 (seven orifice plates). Pressures were measured at wall taps located 1 pipe diam upstream and downstream from the orifice plate, and at corner taps. The coefficients (KY) were computed for each test on the basis of the upstream pressure measured at the pipe wall 1 diam from the plate and on a discharge pressure measured at the corner tap. Each of the seven plates was tested over a range of pressure ratios from unity to about $r = 0.20$. When plotted versus the pressure ratio, the KY-values formed essentially two straight lines for each plate; one line extended from $r = 1.0$ to 0.63, and a second line of increased slope extended from $r = 0.63$ to the limit of the test pressure ratios. The water coefficient K was determined for each plate by extrapolation to unity pressure ratio. The expansion factor-pressure ratio relation was established; the subcritical Y-values showed close agreement with the ASME flange-

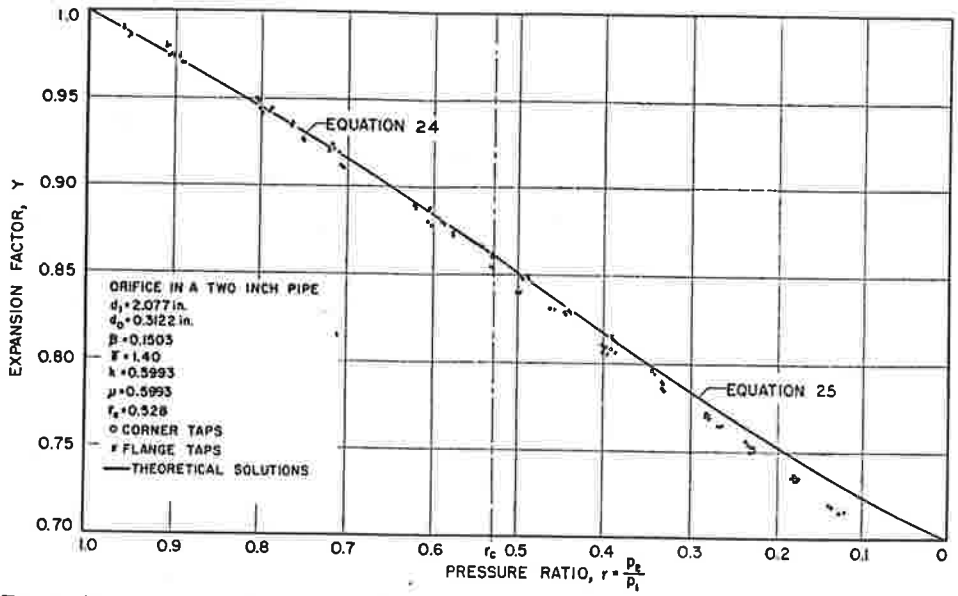

FIG. 8 COMPARISON OF THEORETICAL SOLUTIONS WITH EXPERIMENTALLY DETERMINED EXPANSION FACTORS FOR AIR FLOW IN A 2-IN. PIPE METER (ASME)

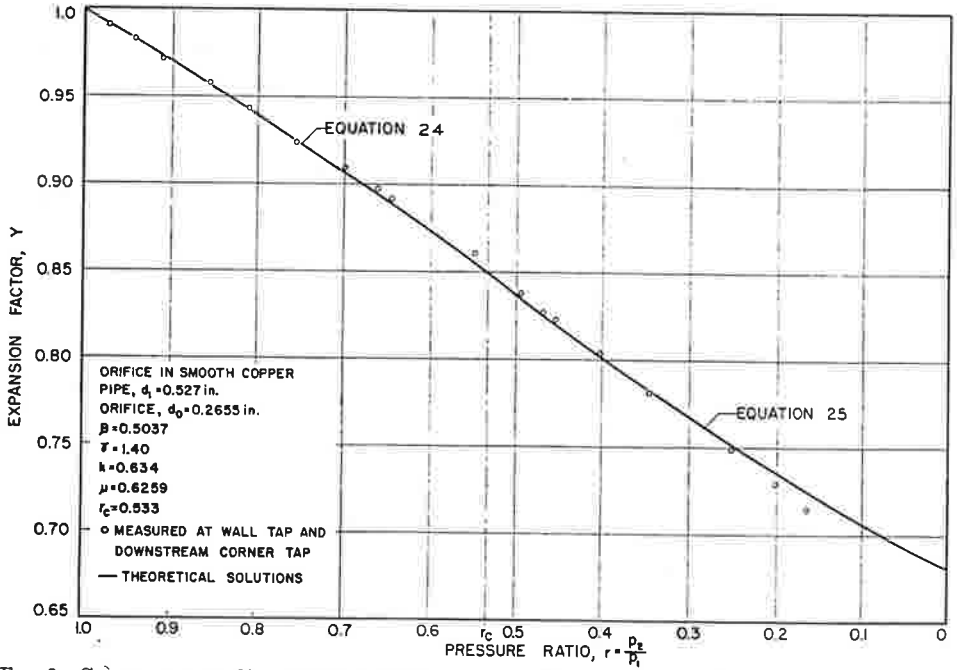

FIG. 9 COMPARISON OF THEORETICAL SOLUTIONS WITH EXPERIMENTALLY DETERMINED EXPANSION FACTORS FOR AIR FLOW IN A 0.527-IN. PIPE METER

tap expansion factors for plates with diameter ratios to 0.7. Expansion-factor equations were presented for the supercritical region.

A theoretical solution for the case of supercritical flow previously presented by the author was compared with air data for orifices with $\beta = 0.15$ and $\beta = 0.50$. The theory agreed with experimental results within 1 per cent for most tests; the difference increased to 2 per cent at very low pressure ratios.

Practical Applications. The square-edged orifice for supercritical flow appears to have the same advantages that have firmly established it as a metering device in the subcritical range of pressure ratios, i.e., simplicity, economy, and ease of reproduction. These factors plus the convenience of the supercritical expansion-factor correlation suggest the use of the orifice in place of the so-called critical-flow nozzle in many applications: the convergent metering nozzle is not infallible, for appreciable variations may occur in the discharge coefficients for flow at high velocities if the nozzle is not properly shaped to avoid wall separation.[8]

Heretofore, the absence of any theoretical solution, and the limited nature of the experimental evidence, have barred effectively the use of the orifice for accurate metering at low pressure

[8] Witte's tests (32), for example, showed that the coefficient of a convergent nozzle changed by as much as 6 to 8 per cent for flow near the critical-pressure ratio.

ratios. Such use has received scant attention in the literature; and the usual attack has been to treat the orifice as a convergent nozzle, i.e., to assume a constant discharge rate in the supercritical range of pressure ratios. Suggested values of discharge coefficients have ranged from 0.60 to 0.86; actually, the adiabatic discharge coefficient varies by about 15 per cent in the supercritical region.

The use of the expansion-factor type of flow equation and the convenient linearity of the Y-r correlation should facilitate the metering of compressible fluids at supercritical pressure ratios with an accuracy comparable to that in the usual metering range.

Acknowledgment

This work was made possible by a graduate fellowship granted by The Pure Oil Company, and aided by a research grant from the Technological Institute of Northwestern University. The author wishes to thank Prof. Edward F. Obert for his valuable help and encouragement during the course of this investigation; Messrs. J. Wagner and G. Sovran gathered certain of the experimental data.

Bibliography

1 "The Flow of Gases at High Speeds," by T. Stanton, Proceedings of the Royal Society, series A, vol. 111, 1926, p. 306.

2 "Abrupt Energy Transformation in Flowing Gases," by N. P. Bailey, Trans. ASME, vol. 69, 1947, p. 749.

3 "Super-Critical Compressible Flow Through Square-Edged Orifices," by R. G. Cunningham, Dissertation, Northwestern University, Evanston, Ill., 1950.

4 "Fluid Meters, Their Theory and Application," Report of the ASME Special Research Committee on Fluid Meters, fourth edition, New York, N. Y., 1937.

5 "Values of Discharge Coefficients of Square-Edged Orifices," by H. Bean, *American Gas Association Monthly*, 1935, p. 259.

6 "The History of Orifice Meters and the Calibration, Construction and Operation of Orifices for Metering," Report of the Joint American Gas Association, ASME Committee on Orifice Coefficients, 1935.

7 "Flow Measurement by Means of Standardized Nozzles and Orifice Plates," Power Test Codes, Part 5, ASME, New York, N. Y., 1940.

8 "Thermodynamic Properties of Air," by R. Gerhardt, F. Brunner, B. Sage, and W. Lacey, *Mechanical Engineering*, vol. 64, 1942, p. 270.

9 "Regeln für die Durchflussmessung mit genormten Düsen und Blenden" ("Regeln"), fourth edition, 1937; available as NACA Technical Memorandum 952, 1940.

10 "Critical Flow Through Sharp-Edged Orifices," by J. A. Perry, Jr., Trans. ASME, vol. 71, 1949, p. 757.

11 "Temperature Measurement," Power Test Codes, Instruments and Apparatus, part 3, ASME, New York, N. Y., 1931.

12 "Thermodynamic Properties of Steam," by J. Keenan and F. Keyes, John Wiley & Sons, Inc., New York, N. Y., 1936.

13 "Überkritische Entspannung kompressibler Flüssigkeiten," by W. Schiller, *Forschung auf dem Gebeite des Ingenieurwesens (Forschung)*, vol. 4, 1933, p. 128.

14 "Recherches experimentales sur la limite de la vittesse que prend un gaz quand il passe d'une pression a un autre plus faible," by G. Hirn, *Annalen de Chimie et de Physik*, sixth series, vol. 7, 1886, p. 289.

15 "The Discharge of Gases Under High Pressure," by L. Hartshorn, Proceedings of the Royal Society of London, series A, vol. 94, 1918, p. 155.

16 "Flow of Steam Through Nozzles," by A. Rateau, D. Van Nostrand Company, Inc., New York, N. Y., 1905.

17 "The Flow of Air and Steam Through Orifices," by H. Reynolds, Trans. ASME, vol. 38, 1916, p. 799.

18 "Super-Critical Compressible Flow Through a Square-Edged Orifice," by R. G. Cunningham, Proceeding of the Midwestern Conference on Fluid Dynamics, vol. 1, University of Illinois, May, 1950, Edward Brothers, Inc., Ann Arbor, Mich., 1951.

19 "The Orifice as a Basis of Flow Measurement," by J. Hodgson, The Institute of Civil Engineers, Selected Engineering Paper 31, 1925.

20 "Performance of Conical Jet Nozzles in Terms of Flow and Velocity Coefficients," by R. Grey and H. Wilsted, NACA Technical Note 1757, 1948. See also Technical Note 1947, 1949.

21 "Flow in Smooth Straight Pipes at Velocities Above and Below Sound Velocity," by W. Frössel, NACA Technical Memorandum 844, 1938.

22 "Die Strömung durch Düsen und Blenden," by R. Witte, *Forschung*, vol. 2, 1931, p. 291.

23 "Gas Jets," by A. Chaplygin, *Scientific Memoirs of the University of Moscow*, vol. 21, 1904, p. 1. Available as NACA Technical Memorandum 1063, 1944.

24 "Durchflusszahlen von Düsen und Stauränder," by R. Witte, *Forschung*, vol. 1, 1930, p. 113. (Volume 1 was published under the title "Technisch Mechanik und Thermodynamik.")

25 "Einfluss der Expansion auf die Kontraktion hinter Staurändern," by G. Ruppel, *Forschung*, vol. 1, 1930, p. 151.

26 "Handbuch der Experimental Physik," Akademische Verlagsgesellschaft, by H. Mueller and H. Peters, M.B.H., Leipzig, Germany, vol. 4, 1931, p. 555.

27 "Notes on the Contraction Coefficient of Jets of Gas," by E. Buckingham, U. S. National Bureau of Standards, *Journal of Research*, vol. 6, 1931, p. 765. See also vol. 9, 1932, p. 61.

28 "Die Strömung von Gasen durch Blenden," by W. Nusselt, *Forschung*, vol. 3, 1932, p. 11.

29 "Expansion Correction of Contraction Coefficients of Orifices," by A. Busemann, *Forschung*, vol. 4, 1933, p. 186. Available in *American Gas Association Monthly*, vol. 15, 1933, p. 476.

30 "Handbuch der Experimental Physik," Akademische Verlagsgesellschaft, by A. Busemann, M.B.H., Leipzig, Germany, vol. 4, 1931, p. 343.

31 "Beitrag zur Messung von Luftmengen," by H. Bachmann, Dissertation, Darmstadt, Germany, 1911.

32 "Die Strömung durch Düsen und Blenden," by R. Witte, *Forschung*, vol. 2, 1931, p. 295.

Discussion

J. A. Perry, Jr.[9] The writer's values of KY in a previous paper[10] are a maximum of 2.2 per cent higher than the author's. This could be due, in part, to the smaller values of β used by the writer.

It will be noted that when values of KY for $\beta > 0.4$, taken from Table 2 and Fig. 6 of the paper, are substituted in Equation [1], that the flow G, increases to a maximum and then decreases with decreasing pressure ratio. This maximum flow value appears between $r = 0.1$ and $r = 0.3$ depending upon β.

It would not seem that decreasing pressure ratio could result in decreasing flow, so there appear to be discrepancies in the values given for KY in Table 2.

The writer indicated that subcritical flow with a negligible velocity of approach could be expressed

$$\Omega = M\sqrt{1 - r^2}$$

where

$$\Omega = \frac{w\sqrt{T}}{PA}$$

where

w = flow, lb per sec
T = upstream temperature, deg R
P = upstream pressure, psia
A = orifice area, sq in.
r = pressure ratio, P_2/P_1
M = const

This equation takes the form of an ellipse. That subcritical flow can be expressed in elliptical form was further shown by Bean, Buckingham, and Murphy[11] as demonstrated by the writer.

[9] Republic Flow Meters Company, Chicago, Ill. Jun. ASME.

[10] "Critical Flow Through Sharp-Edged Orifices," by J. A. Perry, Jr., Trans. ASME, vol. 71, 1949, pp. 757–764.

[11] "Discharge Coefficients of Orifices," by H. S. Bean, E. Buckingham, and P. S. Murphy, National Bureau of Standards, *Journal of Research*, vol. 2, 1929, pp. 561–658 (RPno. 49).

An investigation of the author's subcritical data indicates that the compressible flow function is approximately elliptical for the values of β as given.

Since compressible flow is not a function of pressure differential, as is in compressible flow, but seems to be a function of some other variable, namely, pressure ratio, it would appear that the approach should be from a different angle. Corrections should be on the order of a few per cent, rather than the sizable corrections now employed.

The author is to be congratulated on his paper. The work appears to be quite thorough and is an excellent contribution on a subject about which a minimum of information is available.

Author's Closure

In Table 2 the values of the KY products at zero pressure ratio were, of course, obtained by extrapolation, and are included only to illustrate the method used in constructing the expansion-factor curves in Fig. 7 from the KY plots in Fig. 6.

When plotted as a function of the orifice pressure ratio, the mass flow rate G forms a curve of decreasing slope as lower pressure ratios are encountered. The response of G to a decrease in r at low values of the pressure ratios is quite small, particularly for large diameter ratios. For example, a reduction in pressure ratio from 0.3 to 0.2 results in a mass-flow increase of about 2 per cent for orifice meters of small diameter ratio, and an increase of less than one per cent for large diameter ratios.

Curves representing the mass-flow rates G as functions of the pressure ratio can be constructed from Equation [1] and the KY—r relations presented in Fig. 6. For some of the orifices of larger diameter ratios, this method results in the mass flow G attaining a maximum. For diameter ratios of 0.5, 0.6, and 0.7 (see Fig. 6) this maximum occurs between $r = 0.15$ and 0.10; and every case at a value of r beyond the limit of the experimental data. The decrease in the magnitude of G from this point to $r = 0$ is so small (less than one half of one per cent for $\beta = 0.5$ and 0.6 and about one per cent for $\beta = 0.7$) as to be negligible. This behavior is no doubt a result of the extrapolation and is not surprising, for in this region near zero pressure ratio, a relatively large change in r produces a small change in G that is of the same order of magnitude as the over-all accuracy of the measurement.

The measurement of discharge coefficients for the largest orifice plate, with $\beta = 0.8$, was limited by the apparatus to pressure ratios above $r = 0.464$. The extrapolation of the data for $\beta = 0.8$ beyond the limits indicated in Fig. 6 is unwarranted. If KY or Y values are obtained in this manner, the calculated G—r curve displays a definite maximum between $r = 0.25$ and 0.30. Based upon improper extrapolation, this curve has little, if any, significance.

A flow equation with "corrections . . . . . of the order of a few per cent" exists in the author's theoretical solution (18) which is reviewed in this paper. The solution for the gas-jet contraction coefficient with the isentropic flow Equations [21] and [23] have been shown to predict mass-flow rates quite accurately. It has been pointed out (18) that a small correction factor could be incorporated to enable even closer agreement with experimental results. Similarly, if values of Y_{th} be computed from Equations [24] and/or [25] for use with Equation [1], any small deviations between the theoretical solution and experimental data (see Figs. 8 and 9) could be compensated with an experimentally determined correction factor C. For example

$$G = K(CY_{th})A_0\sqrt{2g_c\rho_1\Delta p} \quad \ldots\ldots\ldots\ldots [27]$$

The term C will depend upon the same variables as Y_{th}, such as r, β, and γ.

There would appear to be little advantage in treating C and Y_{th} separately, other than to evaluate the accuracy of the theoretical prediction. Accordingly, the correlation of experimental data may be simplified without sacrifice of theoretical soundness by treating the product CY_{th}, or Y, instead of the parts.